Modelling Needle Forces during Insertion into Soft Tissue

Conference Paper *in* Conference proceedings: ... Annual International Conference of the IEEE Engineering in Medicine and Biology Society. IEEE Engineering in Medicine and Biology Society. Conference · August 2015

DOI: 10.1109/EMBC.2015.7319477

5 authors, including:

Zhuoqi Cheng
Istituto Italiano di Tecnologia
15 PUBLICATIONS **71** CITATIONS
SEE PROFILE

Manish Chauhan
University of Leeds
16 PUBLICATIONS **14** CITATIONS
SEE PROFILE

Leonardo S. Mattos
Istituto Italiano di Tecnologia
136 PUBLICATIONS **761** CITATIONS
SEE PROFILE

Modelling needle forces during insertion into soft tissue

Zhuoqi Cheng*, Manish Chauhan, Brian L. Davies, Darwin G. Caldwell and Leonardo S. Mattos

***Abstract*— Robot-assisted needle-based surgeries are sought to improve many operations, from brain surgery to spine and urological procedures. Force feedback from a needle can provide important guidance during needle insertion. This paper presents a new modelling method of needle force during insertion into soft tissue based on finite element simulation. This is achieved by analysing the results of a series of needle inserting experiments with different insertion velocities. The forces acting on the needle are then modelled based on the experimental results. A simulation is implemented to verify the designed model.**

I. Introduction

Surgical robots are now commonly used in hospitals for providing better surgical performance. Many studies illustrate that robot-assisted surgery can result in better outcomes compared to manual surgery [1]. One example is medical needle intervention, a common but high challenging technique used for accessing tissue structures. Robot-assisted needle-based surgery has been developed and applied in many operations such as fetal hypoplastic left heart syndrome [2] and brachytherapy seeds implanted inside the prostate [3]. Another example is intravenous operation: patients may be stabbed several times before the needle is successfully inserted and there is often great variation in needle insertion skills among medical personal. To reduce the dependence on skilled technicians, decrease procedure time, and reduce errors during intravenous needle and cannula insertion procedures, Harris *et al*. developed an autonomous intravenous robot called Veebot which is able to insert a hypodermic needle into a pre-selected vein. [4]

For effective performance, an automatic intravenous robot requires feedback for vein targeting, needle localization and needle steering. Needle insertion force is a significant variable since it can imply information about insertion depth and trajectory. It can also help to identify and model different tissue types and provide feedback for precise control during robotic needle insertion by enabling reduced tissue deformation and needle deflection [5]. Previous studies [6] also indicate that needle insertion force shows an obvious drop at the moment when it punctures through the vein wall, which is an useful information for automatic control.

Since information about the forces acting on the needle can play an important role in precise needle insertion control, it is necessary to have an accurate model of such forces to be able to properly design a detection and identification system. In addition, it is desirable to model the magnitude of the insertion force such that it can accurately match the actual measurements [7], especially for applications based on predictive force control. For example, haptic feedback can greatly improve needle-based procedures and in such systems reliable models can be valuable to minimize problems related to inaccurate force measurements or latencies. [8]

In order to understand the force changes on the needle during insertion into homogeneous soft tissue, this paper presents a method for modelling and simulating such forces. A series of needle insertion experiments on bio-mimetic phantoms are conducted. Based on the experimental data, the force acting on the needle is analysed and modelled using a finite element method. This paper is arranged as follows. A needle insertion force model with theoretical analysis is introduced in Section II. In Section III, an experiment is designed and conducted to measure the needle insertion force. The measured force information is then used for the model design in Section IV. In addition, a finite element method is also utilized for the modelling simulation. Discussion and conclusions are provided in Section V.

II. Characterization of Needle Insertion Force

Techniques to model needle insertion force have been explored in previous studies. Brett *et al*. [9] tested the needle insertion force on three material samples, namely, skin layer, fatty/loose muscle tissue and ligamentum flavum. These three components were then combined to obtain the force during the whole insertion procedure. Fukushima and Naemura developed a visualization system to represent the needle tip force using a recursive least squares method and a disturbance observer [10].

Okamura *et al*. [11] used experiments to populate theoretical models of force involving stiffness, friction, and cutting. Their study indicates that the total force acting on the needle f_{needle} can be divided into three variables: cutting force, stiffness force and friction.

$$f_{\text{needle}}(z) = f_{\text{cutting}}(z) + f_{\text{stiffness}}(z) + f_{\text{friction}}(z) \qquad (1)$$

where z is the displacement of the needle tip. Specifically, the cutting force f_{cutting} denotes the force that sustains the tissue fracture during needle insertion while the stiffness

*Corresponding author.

Zhuoqi Cheng is with Department of Advanced Robotics, Fondazione Istituto Italiano di Tecnologia, via Morego, 30, 16163 Genova (Zhuoqi.Cheng@iit.it)

Manish Chauhan, Darwin G. Caldwell, Brian L. Davies and Leonardo S. Mattos are with Department of Advanced Robotics, Fondazione Istituto Italiano di Tecnologia, via Morego, 30, 16163 Genova ({Manish.Chauhan, darwin.caldwell, Leonardo.DeMattos}@iit.it)

Brian L. Davies is with the Mechatronics in Medicine Laboratory, Department of Mechanical Engineering, Imperial College London, London, SW7 2AZ, U.K., and also with Department of Advanced Robotics, Fondazione Istituto Italiano di Tecnologia, via Morego, 30, 16163 Genova (b.davies@imperial.ac.uk)

978-1-4244-9270-1/15/$31.00 ©2015 IEEE

force $f_{\text{stiffness}}$ is the force caused by the tissue's deformation. Friction f_{friction} exists between the needle and tissue due to the tissue's clamping effect. Furthermore, according to their analysis, after puncture of the capsule, the stiffness force becomes zero. Thus, a modified Karnopp friction model is used to describe the friction where the cutting force is described as a constant. The values of cutting force and friction are affected by the needle insertion velocity, but if the velocity is constant during the insertion, these two forces remain constant.

The study of Okamura *et al*. [11] provides a very good framework for understanding the needle insertion forces. However, there are several shortcomings in their model. First of all, the tissue's viscous effect, which is very important during needle insertion, is not emphasized. Secondly, the three force component models are fitted to the experimental results without considering their scientific understanding.

In this paper, previous models are reconsidered and a simulation based on the finite element method is proposed in order to have a better understanding of the forces acting on the needle during insertion. Experiments are first performed to obtain force information on the needle. Subsequently, different force components are analysed and corresponding models are built. The tissue's viscous effect during needle insertion is emphasized. Simulation is then performed to verify the proposed model. Primarily, three assumptions are made for this study:

- Single material and homogeneous phantoms are used to simulate muscle tissue;
- The needle is perpendicular to the tissue surface and moves along its axis;
- Only needle axial force is considered.

III. Needle Insertion Force Measurements

A series of experiments were designed and performed to measure the needle insertion force. Results were used to provide evidence for the modelling in Section IV.

A. Experiment Design

The experiments measured the total force on the needle with respect to the absolute needle displacement. There are two main considerations in this experiment.

The first consideration is that the needle insertion forces are measured with respect to the needle absolute displacement (z in Eq. 1) rather than relative insertion depth, although the relative insertion depth of needle has more physical meaning. However, due to the deformation of the tissue during needle insertion, the relative insertion depth could be not only very difficult to obtain, but also difficult to use. In contrast, the needle's absolute displacement is more straightforward. Hence, the total force f_{needle} on the needle is recorded with the absolute needle displacement z as illustrated in Fig. 1. Here, the experiment is designed with a 15 mm stroke.

Secondly, for each insertion, the velocity is set as a constant in order to maintain a constant fracture force [12]. In addition, the experiment was first tested at very low velocity

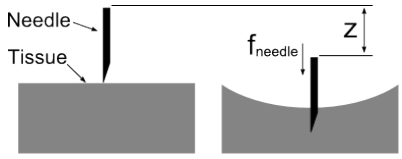

Fig. 1. The experiment is designed to measure the needle insertion force with respect to the absolute needle displacement.

(0.03 mm/s). This was done to minimize the effect of velocity on the insertion force. Subsequently, it was repeated with various insertion velocities (0.3 mm/s, 0.9 mm/s, 1.5 mm/s and 2.1 mm/s) for a better understanding of the influence of velocity on the needle insertion force.

B. Experimental Setup

The experimental setup can be seen in Fig. 2. A servo linear stage (7600-XYZR, Siskiyou Corp., USA) was used to insert the needle into the tissue. A normal hypodermic medical needle (bevel tip, $\phi = 0.9$ mm) was used and attached to an uniaxial force sensor (FSG005WNPB, Honeywell, USA). This force sensor was used to measure the force along the insertion direction which was equivalent to the effective force on the needle. The phantom samples were 30 mm in diameter and 20 mm high. A silicone-based material was used to build a phantom whose mechanical properties are similar to porcine soft tissue (muscle) according to previous studies [13].

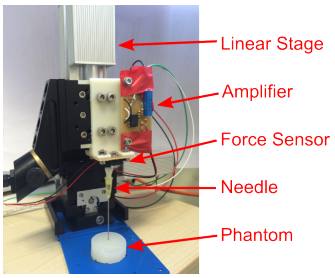

Fig. 2. Experimental set-up for measuring needle insertion force.

C. Experimental Result and Discussion

The experimental results are shown in Fig. 3. The graph shows the total needle insertion force during the whole insertion procedure which starts from the needle tip touching the phantom surface and ends after an absolute displacement downwards of 15 mm. The yellow circle represents the needle insertion force with respect to its displacement in almost static motion (v = 0.03 mm/s), while the red dot, green cross, blue plus and black star represent respectively the results associated to the different insertion velocities of 0.3 mm/s, 0.9 mm/s, 1.5 mm/s and 2.1 mm/s.

According to the results, two conclusions can be drawn. Firstly, the cutting force is shown to be small compared to friction and stiffness force because the needle insertion force does not have an obvious jump when tissue is fractured. This conclusion can be physically understood because the

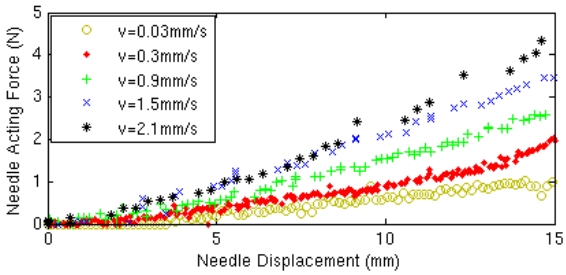

Fig. 3. Experimental results of the needle insertion force

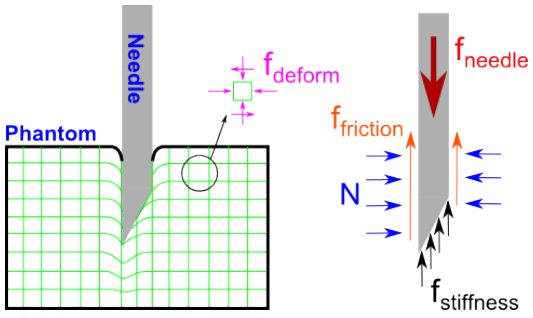

Fig. 4. For the finite element model, f_{deform} represents the stresses on the phantom element during the needle insertion. f_{needle} is considered as the sum of $f_{\text{stiffness}}$ and f_{friction}. $f_{\text{stiffness}}$ is the force acting vertically on the bevel tip due to phantom deformation. Besides, since the phantom is firmly clamping on the needle (N represents the normal force acting on the needle surface), the friction f_{friction} is generated.

diameter of needle is tiny and its bevel is designed to be very sharp so that it ensures effortless tissue cutting. Secondly, besides the fracture force, the needle insertion velocity shows an obvious influence on the friction: the difference between curves under different velocities increases with the insertion depth. This phenomenon can be understood as a viscous friction effect.

IV. MODELLING NEEDLE INSERTION FORCE USING FINITE ELEMENT METHOD

Based on the experimental results above, a new method to understand and simulate the needle insertion force using finite element method is proposed.

A. Modelling of Forces Acting on the Needle

As discussed above, the forces on the needle depend on the insertion velocity into the bio-mimetic phantom. According to the study [11], the needle insertion force f_{needle} can be understood as a combination of force for cutting the phantom f_{cutting}, force for overcoming tissue stiffness $f_{\text{stiffness}}$ and force for resisting the friction f_{friction}. However, since the cutting force barely has a magnitude associated with it, it is neglected in the following simulation and the model becomes:

$$f_{\text{needle}} = f_{\text{stiffness}} + f_{\text{friction}} \tag{2}$$

Here, $f_{\text{stiffness}}$ is defined as the force that results from the reaction force acting on the bevel tip of the needle due to the phantom deformation. The bio-mimetic phantom is a rubber-like hyper-elastic material with similar nonlinear deformation behaviour as human muscle tissues [13]. This is due to the elastic properties of the tissue structure and also to collision with and puncture of the inner structures. As can be seen in Fig. 4, $f_{\text{stiffness}}$ is the force needed to overcome the reaction force on the needle's tip by the deformed phantom.

A finite element mesh is applied to the phantom, and $\{f_{\text{deform}}\}$ is the stress matrix applied to the phantom elements. During needle insertion, the phantom is squeezed by the needle, and the finite element model can be expressed as:

$$[K]\{U\} = \{f_{\text{deform}}\} \tag{3}$$

where $\{U\}$ is the strain matrix of the elements; and $[K]$ is the stress-strain matrix of the phantom. In this paper, the Mooney-Rivlin model is applied [14] for modelling the bio-mimetic phantom. In continuum mechanics, the MooneyRivlin model is commonly used to describe a hyper-elastic material whose strain energy density function is a linear combination of two invariants of the left Cauchy-Green deformation tensor. Based on this model, $f_{\text{stiffness}}$ can be calculated through finite element simulation while the tissue deformation is highly complicated during needle insertion.

f_{friction} is estimated from an understanding of the viscous and damping friction. Since the damping viscous force is a function of the velocity of needle insertion, the two components (static friction and kinetic friction) affect its magnitude. As the needle tries to enter the tissue and penetrate the surface, the stiffness of the tissue surface opposes the needle motion. This opposition force is modelled in the static friction component $f_{\text{s}}(z)$. Meanwhile, as can be observed from the experimental results, the friction force increases with the needle insertion velocity. Hence, there should be another kinetic friction component $f_{\text{k}}(v, z)$ that contributes to the energy dissipation.

$$f_{\text{friction}}(v, z) = f_{\text{s}}(z) + f_{\text{k}}(v, z) = \mu_s N + \mu_k N \tag{4}$$

where μ_s and μ_k are the friction coefficient of the static friction and kinetic friction respectively. In addition, N represents the normal force acting on the needle surface from the phantom surface which can be seen in Fig. 4. This force is perpendicular to the direction of motion of the needle.

Furthermore, to include the sliding velocity between mating surfaces in the kinetic friction, the kinetic friction coefficient can be written as

$$\mu_k = \eta v \tag{5}$$

where the proportionality factor η is known as the damping constant. Thus, Eq. 4 can be written as

$$f_{\text{friction}}(v, z) = (\mu_s + \eta v)N \tag{6}$$

B. Model Construction and Simulation

As specified in the model proposed above, during the needle insertion, the phantom deformation and the normal force N are changing in a complicated way. The finite element method is considered to be a very powerful tool to simulate the proposed needle insertion model. Because

the amount of the cutting force is small, it is ignored in this model. Without the cutting force, the needle penetration can be considered as frictional sliding with the crack propagation neglected. Ansys software is then chosen to construct the model and simulate the combined force of the friction and stiffness force on the needle during insertion.

Fig. 5 shows the 3D modelling of needle and phantom. The 3D model is designed and built as a half portion such that it is possible to implement interference contact between needle and tissue. The phantom model is built as a block with 20 mm long, 10 mm wide and 20 mm height while the needle is modelled as a half section of normal hypodermic needle (diameter: 0.9 mm, bevel tip angle: 20°, length: 20 mm).

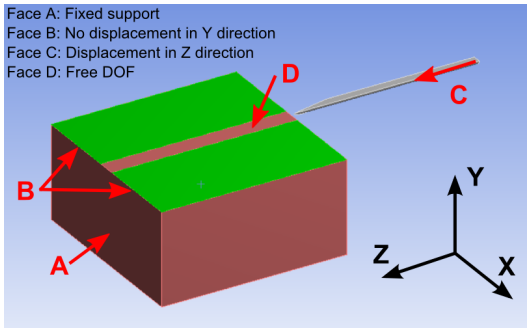

Fig. 5. Finite element model of needle inserting into phantom. The brown block represents the phantom while the silver half cylinder represents the needle. In the Ansys DOF restriction, Face A is set with fixed support. The top surface of the phantom model is splitted into three areas with two green facets (Face B) setting no displacement in Y direction and the middle area (Face D) free of DOF. The rightist section face of the needle model is set with a $15mm$ displacement in Z direction.

As indicated in Fig. 5, the left face of the phantom (A) is a fixed support while the needle (C) can only move along the Z axis and insert into the phantom for 15 mm. The top face of the phantom model is separated into 3 areas. Two areas shown in green (B) are restricted without displacement in Y axis while the remaining middle area (D) is free. The purpose of this design is to make the simulation closer to the real situation. During the simulation of insertion, the needle is immersed into the phantom and the deformed phantom should firmly clamp on the needle. The width of the middle area D is set to be 2 mm in order to ensure result convergence.

As stated above, the phantom model is defined with hyper-elastic material where the Mooney-Rivlin model is applied. Material constant $C10$ and $C01$ is set as 0.8 MPa and 0.16 MPa (silicon soft rubber). Besides, the needle is modelled using structural steel, whose Young's Modulus is 2e5 MPa and Poisson's Ratio is 0.3.

C. Simulation Result

According to the modelling analysis above, the static friction coefficient μ_s is found to be 0.05. In addition, the friction coefficients are changed for the kinetic part with η = 0.08. The red, green, blue and black curves shown in Fig. 6 represent the simulation results of the needle insertion force with different insertion velocities: 0.3 mm/s, 0.9 mm/s, 1.5 mm/s and 2.1 mm/s respectively. Compared to the experimental results in Section III, the simulation of the model confirms that the experimental results are dependent upon the needle insertion velocity.

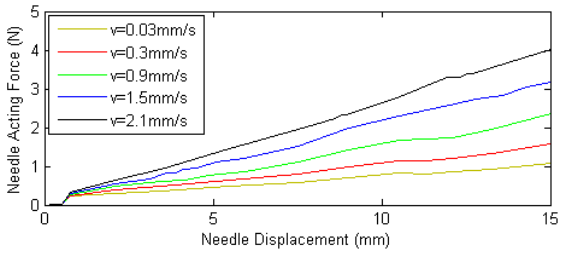

Fig. 6. Simulation results of needle insertion force at different insertion velocities.

V. Discussion and Conclusions

This paper has presented a model design and simulation for understanding the forces acting on the needle during its insertion into homogeneous soft tissue. Finite element simulation and viscous effects are used to model the needle insertion force. A series of experiments were conducted at various insertion velocities. Subsequently, the experimental results are analysed and used for model construction. Then a finite element simulation is presented based on this designed model. The simulation is implemented and demonstrates the validity of this designed model. The conclusion from this modelling and simulation is that by observing the insertion velocity and needle insertion force, the insertion depth of needle can be estimated, which can be highly beneficial in the control of robot-assisted needle insertion surgery. Also the simulation is novel compared to other previous work in that it includes the effects of velocity, giving a closer approximation to measured tissue forces.

Although the simulation matches the experimental results, there are still many aspects of this work that can be improved. Currently, only homogenous bio-mimetic phantoms have been used in the experiment. Animal tissue will be tested in the next step to provide a closer relationship to reality. In addition, some simulation coefficients were designed by trial and error, and in future these will be measured more scientifically. Also, the lateral force on the needle due to its bevel tip effect will be studied in order to improve the design model.

Acknowledgment

The authors would like to thank the technicians from the ADVR department of Istituto Italiano di Tecnologia for their support in manufacturing the test rig in Fig. 2.

References

[1] G. Barresi, N. Deshpande, L. S. Mattos, A. Brogni, L. Guastini, G. Peretti, and D. G. Caldwell, "Comparative usability and performance evaluation of surgeon interfaces in laser phonomicrosurgery," in *Intelligent Robots and Systems (IROS), 2013 IEEE/RSJ International Conference on*. IEEE, 2013, pp. 3610–3615.

[2] M. Heverly, P. Dupont, and J. Triedman, "Trajectory optimization for dynamic needle insertion," in *Robotics and Automation, 2005. ICRA 2005. Proceedings of the 2005 IEEE International Conference on*. IEEE, 2005, pp. 1646–1651.

[3] N. J. Cowan, K. Goldberg, G. S. Chirikjian, G. Fichtinger, R. Alterovitz, K. B. Reed, V. Kallem, W. Park, S. Misra, and A. M. Okamura, "Robotic needle steering: Design, modeling, planning, and image guidance," in *Surgical Robotics*. Springer, 2011, pp. 557–582.

[4] R. J. Harris, J. B. Mygatt, and S. I. Harris, "Systems and methods for autonomous intravenous needle insertion," Patent, Dec. 22, 2011, uS Patent App. 13/335,700.

[5] N. Abolhassani, R. V. Patel, and F. Ayazi, "Minimization of needle deflection in robot-assisted percutaneous therapy," *The international journal of medical Robotics and computer assisted surgery*, vol. 3, no. 2, pp. 140–148, 2007.

[6] A. Zivanovic and B. L. Davies, "A robotic system for blood sampling," *Information Technology in Biomedicine, IEEE Transactions on*, vol. 4, no. 1, pp. 8–14, 2000.

[7] M. H. Saito and T. Togawa, "Detection of needle puncture to blood vessel using puncture force measurement," *Medical and Biological Engineering and Computing*, vol. 43, no. 2, pp. 240–244, 2005.

[8] D. De Lorenzo, Y. Koseki, E. De Momi, K. Chinzei, and A. M. Okamura, "Experimental evaluation of a coaxial needle insertion assistant with enhanced force feedback," in *Engineering in Medicine and Biology Society, EMBC, 2011 Annual International Conference of the IEEE*. IEEE, 2011, pp. 3447–3450.

[9] P. N. Brett, T. Parker, A. J. Harrison, T. A. Thomas, and A. Carr, "Simulation of resistance forces acting on surgical needles," *Proceedings of the Institution of Mechanical Engineers, Part H: Journal of Engineering in Medicine*, vol. 211, no. 4, pp. 335–347, 1997.

[10] Y. Fukushima and K. Naemura, "Estimation of the friction force during the needle insertion using the disturbance observer and the recursive least square," *ROBOMECH Journal*, vol. 1, no. 1, pp. 1–8, 2014.

[11] A. M. Okamura, C. Simone, and M. D. O'Leary, "Force modeling for needle insertion into soft tissue," *Biomedical Engineering, IEEE Transactions on*, vol. 51, no. 10, pp. 1707–1716, 2004.

[12] M. Mahvash and P. E. Dupont, "Mechanics of dynamic needle insertion into a biological material," *Biomedical Engineering, IEEE Transactions on*, vol. 57, no. 4, pp. 934–943, 2010.

[13] Y. Wang, B. L. Tai, H. Yu, and A. J. Shih, "Silicone-based tissue-mimicking phantom for needle insertion simulation," *Journal of Medical Devices*, vol. 8, no. 2, p. 021001, 2014.

[14] I.-S. Liu, "A note on the mooney–rivlin material model," *Continuum Mechanics and Thermodynamics*, vol. 24, no. 4-6, pp. 583–590, 2012.